A Powertrain Model for Real-Time Vehicle Simulation

Zhenhui Yao
Department of Mechanical, Industrial and Manufacturing Engineering
The University of Toledo
Toledo, OH 43606-3390
zyao@eng.utoledo.edu

Ric Mousseau
Department of Mechanical, Industrial and Manufacturing Engineering
The University of Toledo
Toledo, OH 43606-3390
ric.mousseau@eng.utoledo.edu

Ben G. Kao
Ford Research Laboratories
Ford Motor Company
Dearborn, MI 48121-2053
bkao@ford.com

ABSTRACT

Realistic driving simulation requires adequate reproduction of powertrain dynamic response. Interaction between the powertrain and the vehicle will influence the vehicle ride response and can affect the smoothness of the powertrain during throttle application. As a vehicle travels down the road, unevenness in the road causes the powertrain to vibrate. This vibration causes the drive torque to vary and to produce inertial forces that disturb the vehicle body. The simulation model described in this paper includes both types of interactions. It uses a lumped parameter approach to reproduce the torque produced by the powertrain system. Rigid body motion of the powertrain is defined through user prescribed modal properties (i.e., natural frequencies and mode shape coefficients). This paper describes the powertrain model and briefly describes the vehicle dynamics model. Simulation results for a front wheel drive vehicle are presented and the sensitivity of the model to key input parameters is examined.

INTRODUCTION

Realistic driving simulation requires adequate reproduction of powertrain dynamic response. Interaction between the powertrain and the vehicle will influence the vehicle ride response and can affect the smoothness of the powertrain during throttle application. As a vehicle travels down the road, unevenness in the road causes the powertrain to vibrate. This vibration causes the drive torque to vary and to produce inertial forces that disturb the vehicle body. The simulation model described in this paper includes both types of interactions. It uses a lumped parameter approach to reproduce the torque produced by the powertrain system. Rigid body motion of the powertrain is defined through user prescribed modal properties (i.e., natural frequencies and mode shape coefficients).

Power in a ground vehicle is generated by the engine and transmitted through the drivetrain system. For a typical front wheel drive (FWD) vehicle equipped with an automatic transmission, the powertrain system encompasses the following major parts: engine, torque converter, transmission gear set, final drive and differential. Driveshafts provide flexible connection between the powertrain and drivewheels and suspensions. The powertrain interacts with the vehicle dynamically in the following ways:

1. Engine power (torque and speed) passes through powertrain system and driveshafts to drivewheels. The driveshafts apply torques to the drive wheels to move the vehicle, and equal and opposite, reaction moments are applied on the powertrain body.

2. Powertrain assembly is mounted to the chassis via compliant mounts. The powertrain and the chassis interact via the mounts.

3. Vibrational forces induced into the powertrain and unsprung masses by changes in drive shaft (i.e., constant velocity joints) geometry and friction.

A simple way to model a powertrain mount is to use a network of parallel linear, or nonlinear, springs and dampers that act in x, y and z directions without any coupling. The problems with this method lie in: 1) the difficulty in generating accurate mount data, 2) the lack of force coupling between the x, y and z directions, and 3) the influence of the local subframe deformation, which will affect the behavior of the overall mounts system. A design-target-oriented approach is adopted for modeling powertrain rigid body dynamics. In this method, the powertrain modal properties (i.e., natural frequencies and mode shape coefficients) are regarded as one of the design targets for powertrain system. Rigid body motion of the powertrain is defined using modal analysis. The advantage of this approach is that the mount data is not required and it also offers some reduction in calculation time.

This paper describes a simple and efficient real-time powertrain model for use in a driving simulator. The subject vehicle is a FWD middle-size passenger car, equipped with an automatic transmission, open differential, and 4-wheel independent suspension. The modal method is used to describe the powertrain rigid body dynamics. A lumped parameter torque/speed model is used to describe the powertrain torsional dynamics. The impact of drive shaft friction on the vehicle dynamic response is not addressed in this paper. The reminder of this paper is organized as follows. Modal analysis theory is briefly reviewed and the vehicle model and its major components are described. Simulation results for an example car accelerating straight ahead and for a parametric study are also presented. The final section describes conclusions and future work.

MODAL DYNAMIC ANALYSIS

A linear dynamic mechanical system can be represented by:

$$\mathbf{M}\ddot{\mathbf{d}} + \mathbf{C}\dot{\mathbf{d}} + \mathbf{K}\mathbf{d} = \mathbf{f} \tag{1}$$

Where $\mathbf{M}$ is the mass matrix, $\mathbf{K}$ is the stiffness matrix, $\mathbf{C}$ is the damping matrix, $\mathbf{f}$ is the external force vector, and $\mathbf{d}$ is the displacement vector in physical coordinates. Note that in this paper, upper and lower case bold characters, respectively, describe matrices and vectors. We define a modal matrix $\boldsymbol{\phi}$ whose column vectors are eigenvectors of the system, normalized with respect to the mass matrix, an identity matrix $\mathbf{I}$, and a diagonal matrix $\boldsymbol{\Omega}^2$ whose entries are eigenvalues, i.e., squares of natural frequencies of the system.

$$\boldsymbol{\phi}^t \mathbf{M} \boldsymbol{\phi} = \mathbf{I} \tag{2}$$

$$\boldsymbol{\phi}^t \mathbf{K} \boldsymbol{\phi} = \boldsymbol{\Omega}^2 \tag{3}$$

The displacement vector $\mathbf{d}$ can be expressed as the linear combination of the eigenvectors.

$$\ddot{\mathbf{d}} = \boldsymbol{\phi}\ddot{\mathbf{z}} \qquad \dot{\mathbf{d}} = \boldsymbol{\phi}\dot{\mathbf{z}} \qquad \mathbf{d} = \boldsymbol{\phi}\mathbf{z} \tag{4}$$

Where $\mathbf{z}$ is the generalized coordinates measured in the modal space. Using modal coordinate vector $\mathbf{z}$, Eq. (1) can be expressed in a diagonal form as:

$$\ddot{\mathbf{z}} + \mathbf{C}_\phi \dot{\mathbf{z}} + \boldsymbol{\Omega}^2 \mathbf{z} = \mathbf{f}_\phi \tag{5}$$

Where

$$\mathbf{C}_\phi \;=\; \mathbf{\Phi}^t \mathbf{C} \mathbf{\Phi} \tag{6}$$

$$\mathbf{f}_\phi \;=\; \mathbf{\Phi} \mathbf{f} \tag{7}$$

Usually the matrix $\mathbf{C}_\phi$ in Eq. (6) is not a diagonal matrix, however, it can be diagonalized if proportional damping (1), or modal damping assignment (1), is used to describe the system damping matrix $\mathbf{C}$ approximately.

VEHICLE DYNAMICS MODEL

The vehicle dynamics model is comprised of the sprung mass, unsprung mass, tire model, powertrain rigid body dynamics model, and the powertrain torque/speed model. The interaction between these models is illustrated in Fig. 1. AutoSim (2), a multibody symbolic code generator was used to generate the dynamic simulation program. By using a multibody system description, AutoSim derives equations of motion in terms of ordinary differential equations, and generates a computer source program either in C or Fortran to solve them. Depending on the type of multibody system, and number of degrees of freedom (DOF), the resulting source code is well suited for real-time simulation applications. The components of the vehicle model, powertrain rigid body dynamics model, and torque/speed model are described below.
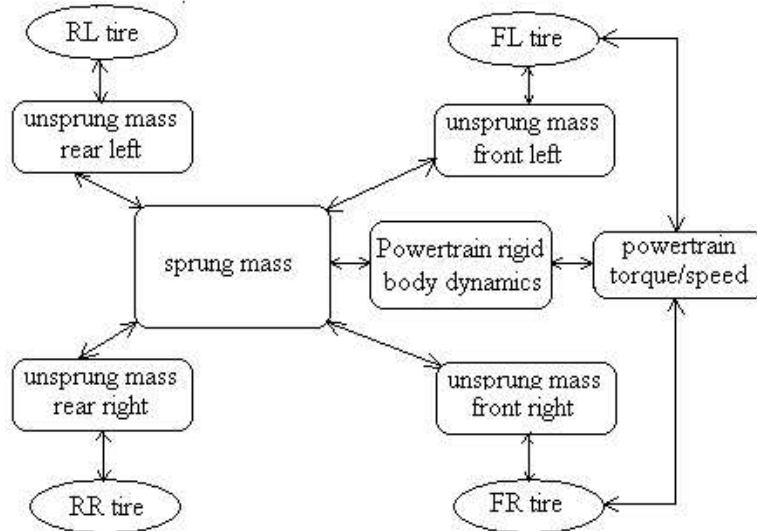

FIGURE 1 Vehicle dynamics model structure

Sprung and Unsprung Masses

The vehicle dynamics model is described in more detail in (3, 4). In this model, we define sprung mass as the assembly of the chassis, the payload, and the proportion of suspension mass that moves with the vehicle body. The sprung mass is represented by a single rigid body that has 6 degrees of freedom (DOFs), i.e., rotations around the roll, pitch, yaw directions, and translations in the longitudinal, lateral and vertical directions. We define the unsprung mass to be the collection of the wheel and brake masses, and the proportion of moving suspension mass. Every unsprung mass can move in the following directions with respect to the sprung mass:

- longitudinal (wheelbase change)
- lateral (track change)
- vertical (suspension rebound and jounce)
- roll (wheel camber)
- yaw (wheel toe-in or toe-out)
- pitch (wheel caster)

We assume that every unsprung body moves along a prescribed path that depends on the vertical movement of the unsprung mass. This path can be determined experimentally, or with a simulation model of the suspension linkage. Deformation of the suspension caused by spindle forces, e.g., compliance steer, is also taken into account. These characteristics are introduced into the model with constraint equations. For instance, the longitudinal position constraint equation for an unsprung mass is:

$$\delta_x(z) + \Delta x - x = 0 \qquad (8)$$

Where, Δx is the wheelbase change due to static compliant deformation, z is the suspension jounce travel, $\delta_x(z)$ is the wheelbase change due to the suspension jounce or rebound, and x is the total wheelbase change.

The springs, shock absorbers and roll stabilizers produce forces that act between the sprung and unsprung masses. Every spring is characterized by a 3rd order polynomial that is a function of suspension displacement. Every shock absorber is characterized by a 3rd order polynomial, with different coefficients for the rebound and jounce directions, that is a function of velocity. Roll stabilizers are modeled as pairs of forces that act, in an equal and opposite fashion, on the sprung and unsprung masses.

Tire Model

The tire model includes a handling component, which is designed to simulate cornering, and traction forces, and an enveloping component (5), which is designed to simulate impact forces. The former uses an algorithm developed by Pacejka (6), and modified by Iowa State University (ISU) to better represent stationary tire behavior. The ISU tire model incorporates wheel spin dynamics and calculates tire dynamic longitudinal and lateral relaxation (7,8). As a tire rolls over a small obstacle, it tends to envelop it and create longitudinal, lateral, and vertical tire forces. The enveloping tire model (ETM) was developed to predict both the longitudinal and vertical tire force as well as deformed tire radius. The vertical enveloping force and the deformed tire radius are used as input to the handling component. The longitudinal enveloping force is combined with the tractive tire force to produce the total longitudinal tire force.

Powertrain Rigid body Dynamics Model

Assuming that the powertrain body only rotates infinitesimally with respect to the sprung mass, the powertrain rigid body system dynamic equations can be expressed in the form of Eq. (1). If further assumptions are made, the powertrain dynamics can also be expressed in modal form.

Kinematics

In Fig. 2, point **P** is the center of gravity (CG) of the powertrain body and the origin of the body coordinates. **P'** denotes the point which is fixed to the chassis body and initially coincides with point **P**. Frame $\mathbf{X_bY_bZ_b}$ describes the body coordinates of the sprung mass and frame **XYZ** denotes the fixed global coordinates. ρ_r denotes the vector **P'P**, viewed in the moving frame $\mathbf{X_bY_bZ_b}$. $\dot{\rho}_r$ and $\ddot{\rho}_r$, respectively, are the velocity and acceleration of point **P**, observed in the moving frame $\mathbf{X_bY_bZ_b}$.

The absolute velocity of point P (9) is

$$\mathbf{v_p} = \mathbf{v_{p'}} + \mathbf{v_{p/p'}} = \mathbf{v_{p'}} + \dot{\rho}_r + \omega_b \times \rho_r \qquad (9)$$

Where $\mathbf{v_{p'}}$ is the absolute velocity of point P', $\mathbf{v_{p/p'}}$ is the relative velocity of point P with respect to point P' and ω_b is absolute angular velocity of the sprung mass. The absolute acceleration of point P (9) is

$$\mathbf{a_p} = \mathbf{a_{p'}} + \mathbf{a_{p/p'}} = \mathbf{a_{p'}} + \dot{\omega}_b \times \rho_r + \omega_b \times (\omega_b \times \rho_r) + 2\omega_b \times \dot{\rho}_r + \ddot{\rho}_r \qquad (10)$$

Where $\mathbf{a}_{p'}$ is absolute acceleration of point **P'**, $\mathbf{a}_{p/p'}$ is the relative acceleration of point **P** with respect to point

P', $\ddot{\omega}_{\mathbf{b}}$ is absolute angular acceleration of the sprung mass.

The relative angular displacement, velocity and acceleration of the powertrain body, with respect to the sprung

mass, are denoted respectively as θ_r, $\dot{\theta}_r$ and $\ddot{\theta}_r$. Assuming infinitesimal rotation, the powertrain body absolute angular velocity is:

$$\dot{\omega}_{\mathbf{p}} = \dot{\omega}_{\mathbf{b}} + \dot{\omega}_{\mathbf{p/b}} = \dot{\omega}_{\mathbf{b}} + \dot{\theta}_r \qquad (11)$$

Where $\dot{\omega}_{\mathbf{p/b}}$ is the relative angular velocity of the powertrain with respect to the sprung mass. The powertrain body absolute angular acceleration is given by:

$$\ddot{\omega}_{\mathbf{p}} = \ddot{\omega}_{\mathbf{b}} + \ddot{\omega}_{\mathbf{b/p}} = \ddot{\omega}_{\mathbf{b}} + \ddot{\theta}_r \qquad (12)$$

Where $\ddot{\omega}_{\mathbf{b/p}}$ is the relative angular velocity of the powertrain with respect to the sprung mass.
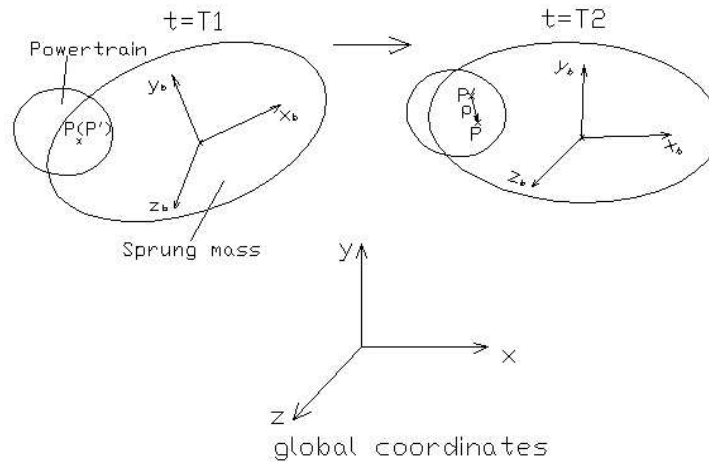
FIGURE 2 Coordinate systems

Dynamics

From Euler Equation (9), Newton's Second Law (9), and Eqs. (9) through (12), we obtain the dynamic equations of motion for the powertrain rigid body.

$$\mathbf{M}\ddot{\mathbf{d}} + \mathbf{C}\dot{\mathbf{d}} + \mathbf{K}\mathbf{d} = \mathbf{f} \qquad (13)$$

$$\mathbf{M} = \begin{bmatrix} \mathbf{M_p} & \mathbf{0} \\ \mathbf{0} & \mathbf{I_p} \end{bmatrix} \qquad (14)$$

$$\mathbf{d} = \begin{Bmatrix} \theta_r \\ \theta_r \end{Bmatrix} \qquad \dot{\mathbf{d}} = \begin{Bmatrix} \dot{\theta}_r \\ \dot{\theta}_r \end{Bmatrix} \qquad \ddot{\mathbf{d}} = \begin{Bmatrix} \ddot{\theta}_r \\ \ddot{\theta}_r \end{Bmatrix} \qquad (15)$$

$$\mathbf{f_1} = \mathbf{M_p}(\mathbf{a}_{p'} + \ddot{\omega}_{\mathbf{b}} + \theta_r + \dot{\omega}_{\mathbf{b}} \times (\dot{\omega}_{\mathbf{b}} + \dot{\theta}_r) + 2\dot{\omega}_{\mathbf{b}} \times \dot{\theta}_r) + \mathbf{C_1}(\dot{\omega}_{\mathbf{b}} + \dot{\theta}_r) \qquad (16)$$

$$\mathbf{f_2} = \mathbf{I_p}\ddot{\omega}_{\mathbf{b}} + \dot{\omega}_{\mathbf{p}} \times (\mathbf{I_p}\dot{\omega}_{\mathbf{p}}) \qquad (17)$$

$$\mathbf{f} = \mathbf{f_e} + \mathbf{f_i} \qquad \mathbf{f_e} = \begin{Bmatrix} \mathbf{f_{e1}} \\ \mathbf{f_{e2}} \end{Bmatrix} \qquad \mathbf{f_i} = \begin{Bmatrix} \mathbf{f_1} \\ \mathbf{f_2} \end{Bmatrix} \tag{18}$$

where $\mathbf{M_p}$ is the 3x3 mass matrix of the powertrain, $\mathbf{I_p}$ is the 3x3 inertia matrix of the powertrain, $\mathbf{C}$ is the 6x6 damping matrix, $\mathbf{C_1}$ is 3x3 sub-matrix of $\mathbf{C}$, $\mathbf{K}$ is the 6x6 stiffness matrix, $\mathbf{f_{e1}}$ and $\mathbf{f_{e2}}$ are the externally applied forces and moments. In this paper, powertrain reaction moment is included as a component of the external moment $\mathbf{f_{e2}}$. The calculation of the reaction moment is defined in next section – Powetrain Torque/Speed Model. $\mathbf{f_e}$ could also be an engine shaking force due to residual unbalance, which is ignored in this study.

Since $\mathbf{f_i}$ depends upon system state variables, Eq. (13) is not an entirely linear equation, and therefore, it needs to be linearized before using modal method to calculate dynamic response of the powertrain rigid body. This is accomplished in Eq. (19) below by lagging $\mathbf{f_i}$ by one integration time step.. This will cause $\mathbf{f_i}$ to behave like an external force vector. Since the time step was already constrained by other dynamics in the model, numerical experiments with the simulation showed the time lag did not adversely affect the solution.

$$\left\{ \mathbf{M}\ddot{\mathbf{d}} + \mathbf{C}\dot{\mathbf{d}} + \mathbf{K}\mathbf{d} \right\}_n = \{\mathbf{f_e}\}_n + \{\mathbf{f_i}\}_{n-1} \tag{19}$$

Modal analysis model

Eq. (5) can be rewritten as

$$\ddot{\mathbf{z}} + \Omega^2 \mathbf{z} = \mathbf{f_\phi} - \mathbf{C_\phi}\dot{\mathbf{z}} \tag{20}$$

The advantage of modal dynamic analysis is that the damping matrix $\mathbf{C_\phi}$ in Eq. (5) is diagonal and the system is uncoupled in modal space. However, this system consists of general viscous damping, and thus, $\mathbf{C_\phi}$ cannot be diagonalized in the modal space $\mathbf{z}$. Since damping plays an important role in the system, approximation methods, e.g., proportional damping, or modal damping assignment method, cannot represent the system damping accurately. Note that if we assume the velocity vector does not change much during the time step, the damping forces can be lagged by one time step, and treated as externally applied forces, thereby decoupling the system.

$$\left\{ \ddot{\mathbf{z}} + \Omega^2 \mathbf{z} \right\}_n = \{\mathbf{f_{i\phi}} - \mathbf{C_\phi}\dot{\mathbf{z}}\}_{n-1} + \{\mathbf{f_{e\phi}}\}_n \tag{21}$$

The powertrain rigid body mode shape coefficients and natural frequencies for the example car are illustrated in Fig. 3. The labels 1 to 6 on vertical axes correspond, respectively, to fore/aft, lateral, and vertical translations and pitch, roll, and yaw rotations. Modal kinetic energy distributions (10) of the powertrain were calculated and listed in Table 1. The modal kinetic energy distributions are used for mode shape identification. For example, in mode 1, lateral, vertical and pitch motions are highly coupled, and in mode 3, the fore/aft motion is dominant and is largely decoupled from other motions.

TABLE 1 Modal Kinetic Energy Distribution

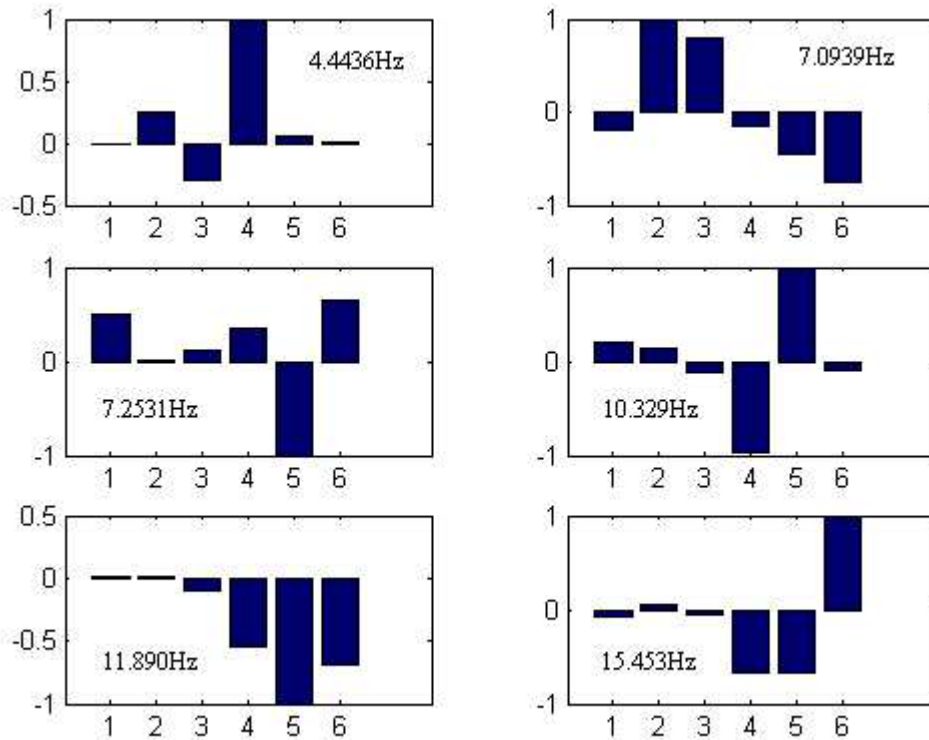| Mode	Frequency (Hz)	Kinetic energy percentage distribution (x100%)					
		Fore/aft	lateral	Vertical	Pitch	Roll	Yaw
1	4.4436	0.004	28.970	41.401	29.410	0.150	0.064
2	7.0939	2.003	58.140	36.599	0.089	0.764	2.395
3	7.2531	71.724	0.030	3.991	3.709	13.701	6.845
4	10.329	19.602	9.686	6.254	34.130	30.110	0.218
5	11.890	0.307	0.176	9.150	13.760	42.809	33.798
6	15.453	6.358	2.919	2.496	18.794	12.771	56.661

FIGURE 3 Powertrain mode shapes and natural frequencies

Powertrain Torque/Speed Model

The torsional dynamics of the powertrain are described with a lumped parameter, one-dimensional model. This model describes the applied engine torques and angular speeds transmitted through all the powertrain components, which consist of the engine, torque converter, transmission gear set, final drive and differential. In the current model, we ignore the transmission rotational inertias, compliances, and damping forces.

Engine Cranktrain

The cranktrain in an IC engine, which includes the crankshafts, connecting rods, and pistons, is lumped as a whole into a one-dimensional rigid-body torsional DOF. The dynamic equation for the cranktrain is described by the following equation.

$$I_e \, \ddot{\theta}_e = T_e - T_p \qquad\qquad (22)$$

Where T_e is the engine brake torque applied on the engine crankshaft, T_p is the torque absorbed by torque converter, and $\ddot{\theta}_e$ is the cranktrain angular acceleration.

We assume the engine torque T_e is generated from a quasi-static 2-D engine map (11), as illustrated in Fig. 4. This map relates engine speed and throttle input to the engine brake torque T_e. This method neglects both the engine firing pulsation and the effect of cranktrain inertia variation. For an automatic transmission vehicle, the engine torque pulsation is largely damped out by the torque converter (11), which supports the aforementioned simplification.
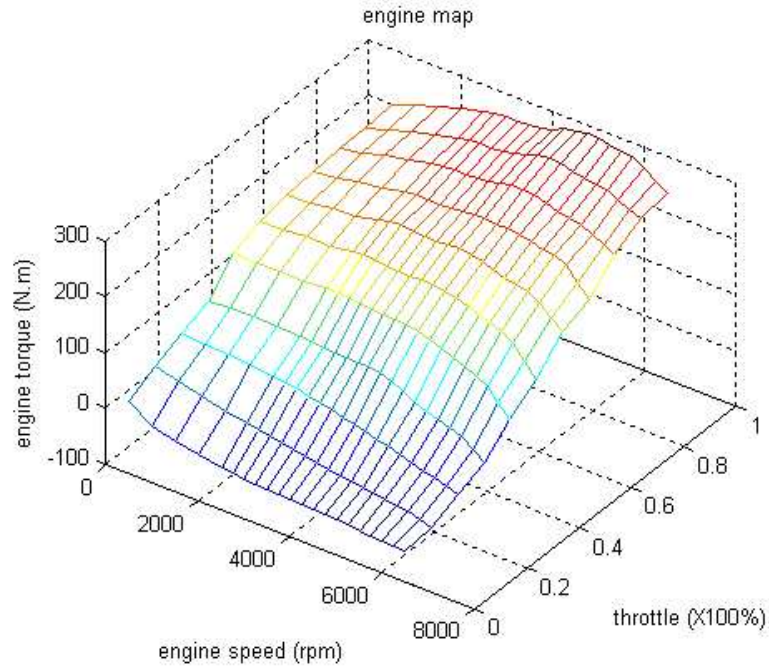
FIGURE 4 Static engine map for the example car

Torque Converter

The torque converter in an automatic transmission performs the following functions: 1) it provides a fluid coupling between the engine and the transmission; 2) it produces torque magnification during the vehicle breakaway stage; 3) it damps out shocks and pulsations present in the engine torque. The following quasi-static relationships are used to describe the relationship between and torque, engine speed, and transmission speed (11).

$$s = \frac{\omega_t}{\omega_p} \qquad\qquad (23a)$$

$$T_p = \frac{\omega_p^2}{C_f^2} \qquad\qquad (23b)$$

$$T_t = C_r T_p \qquad\qquad (23c)$$

where T_t is the output torque, s is speed ratio, C_f is the capacity factor, which is a function of s, as shown in Fig. 5, C_r is the torque ratio, which is a function of s, as shown in Fig. 6, ω_p is input speed, equal to engine speed ω_e, and ω_t is the output speed of the torque converter.
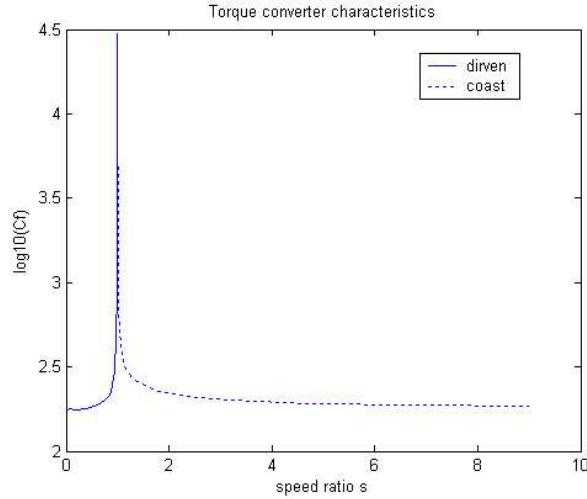
FIGURE 5 Capacity factor of the example torque converter
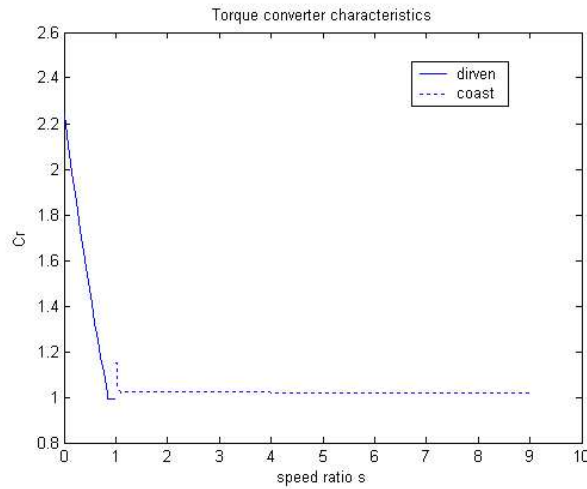
FIGURE 6 Torque ratio of the example torque converter

Transmission Gear Set

The transmission gear set is assumed to be rigid and completely efficient. The following torque and speed relationships hold.

$$T_t = NT_d \qquad\qquad (24a)$$

$$\omega_d = N\omega_t \qquad\qquad (24b)$$

Where N is gear ratio, described in Table 2, T_d and ω_d are output torque and speed from the transmission gear set.

TABLE 2 Gear Ratios of the Example Gear Set

Gear	N
1	2.771
2	1.534
3	1.0
4	0.694
reverse	-2.26

For an automatic transmission, gear shifting is triggered automatically when the vehicle speed exceeds or falls below the threshold values. In this model, the gear shift logic is defined through predefined look-up tables (12), as illustrated in Fig. 7. Since gear shifting does not happen instantly, a one second shift period is assumed. During this period, the torque ratios and the speed ratios are blended linearly over time, to smooth the gear shifting process.

Final drive and differential

The final drive in the differential provides further speed reduction. An open type differential is in the example car powertrain. The open differential requires the input speed to be average speed of the right and left drivewheels times the final drive ratio. It also splits torque equally to left and right side drive wheels (12).

$$\omega_d = N_{fd} \frac{(\omega_l + \omega_r)}{2} \quad\quad\quad (25a)$$

$$T_l = T_r = N_{fd} \frac{T_d}{2} \quad\quad\quad (25b)$$

Where, N_{fd} is the final drive ratio, T_l and T_r represent output torques to left and right drive wheels, ω_l and ω_r are spin speeds of left and right drive wheels. The final drive ratio for the example car is 3.47.
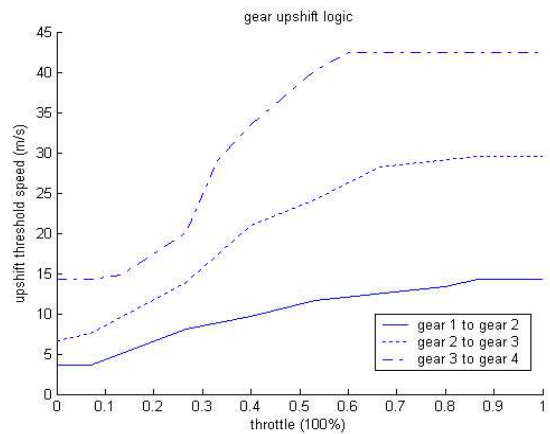
(a)
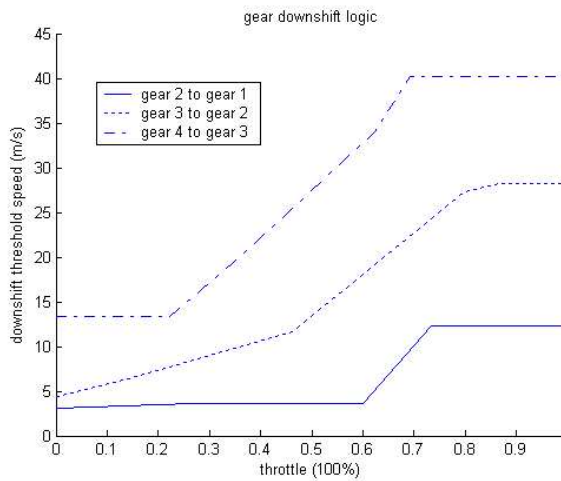
(b)

FIGURE 7 (a) Gear upshift logic and (b) Gear downshift logic

Powertrain reaction moment

While the powertrain outputs torques to drive the vehicle, a reaction moment T_{react} is applied on powertrain body (13), which works as the connection between the powertrain rigid body dynamics and the powertrain torque/speed model.

$$T_{react} = -(I_e \dot{\omega}_e - T_l - T_r) \tag{26}$$

SIMULATION RESULTS AND PARAMETRIC STUDY

Straight Forward Acceleration – Constant Throttle Input

To evaluate the comprehensive vehicle model described above, a simulation of the example car accelerating straight ahead was performed. Table 3 describes the parameters used in the simulation and the resulting execution speeds. The simulation ran slightly slower than real-time on a slow, by today's standards, 700 MHz PC. This model will run in real-time, or faster, on virtually any PC that purchased off the shelf in 2003. The results are shown in Figs. 8 through 11 and these results compare favorably to Salaani's (11) simulation results for a 1994 Ford Taurus. Fig. 8 shows that during the initial stage, the vehicle reaches a peak value of acceleration of 0.38g and then decreases to 0.05g after 40s acceleration. Fig. 9 shows the engine speed keep within 2000~2500RPM except for the initial breakaway stage. Fig. 10 shows during this period, the transmission shifts from 1st gear through 4th gear. Fig. 11 shows that after 40 seconds of constant throttle acceleration (30%), the vehicle achieves a speed of around 33m/s.

TABLE 3 Simulation Parameters and Speed Performances

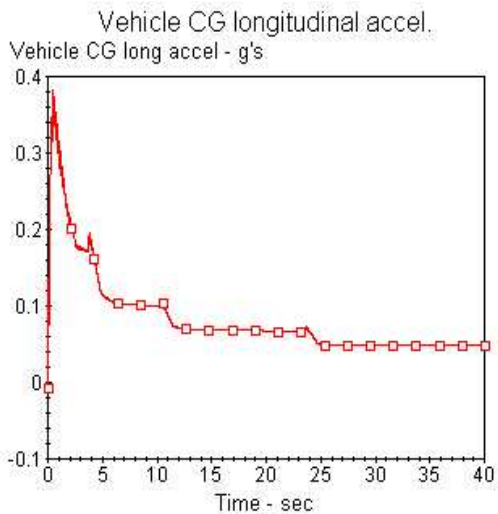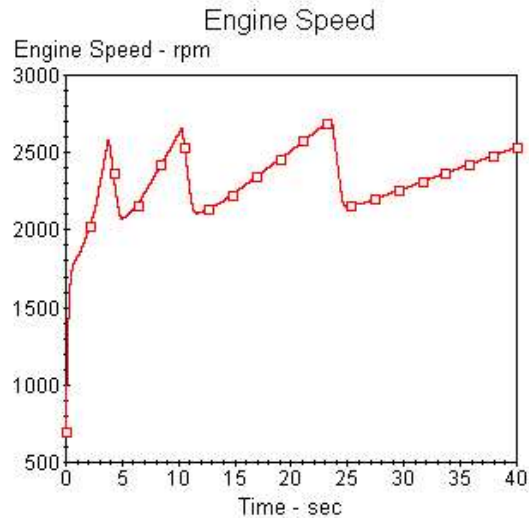|	
Initial Speed	0m/s
Initial Gear	1st
Engine Idle Speed	700RPM
Normalized Throttle Input	30%
Simulation Time Span	40s
Integration Step Size	0.001s
Simulation Platform	Dell PC, PIII 700MHz, Windows 2000 OS
Simulation Speed	1.475s CPU time for per simulated second

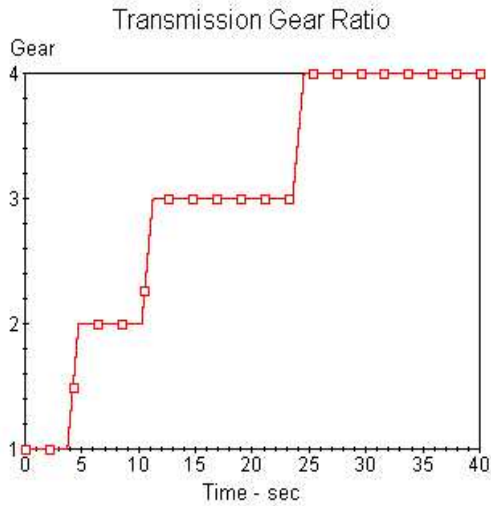**FIGURE 8 Vehicle longitudinal acceleration**   **FIGURE 9 Engine speed**

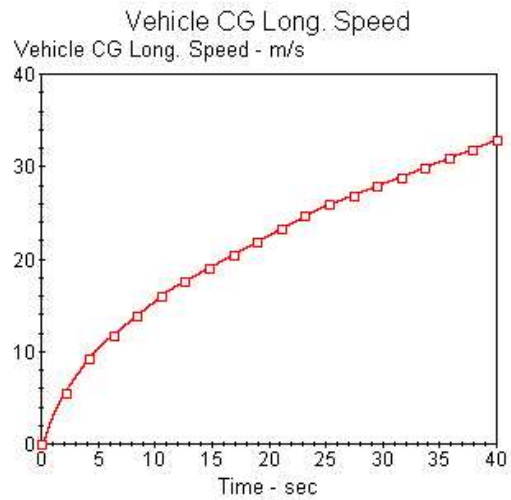**FIGURE 10 Transmission gear ratio**

FIGURE 11 Vehicle longitudinal velocity

Straight Forward Acceleration – Throttle Tip-in

Throttle tip-in refers to the sudden increase in throttle input, i.e., a step throttle input, as illustrated in Fig. 12. Similar to the previous simulation, the tip-in simulation started while the vehicle was stationary. The acceleration response at the driver location is shown in Fig. 13. Note that after tip-in, which occurs at t=3s, there is some overshoot in the vehicle longitudinal acceleration. Motion of the powertrain on its mounts is coupled into the dynamic response of the vehicle. These small-magnitude fluctuations in accelerations due to vibration of the powertrain after tip-in are observed in the enlarged view in Fig. 14.
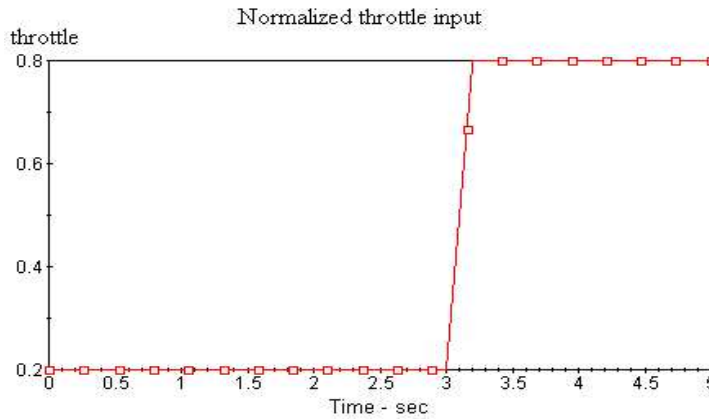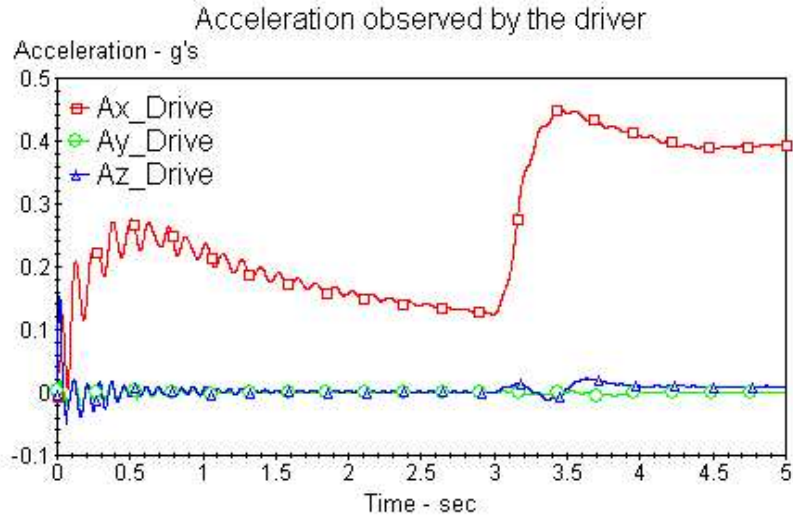

FIGURE 12 Normalized throttle input

FIGURE 13 Tip-in response at the driver's location

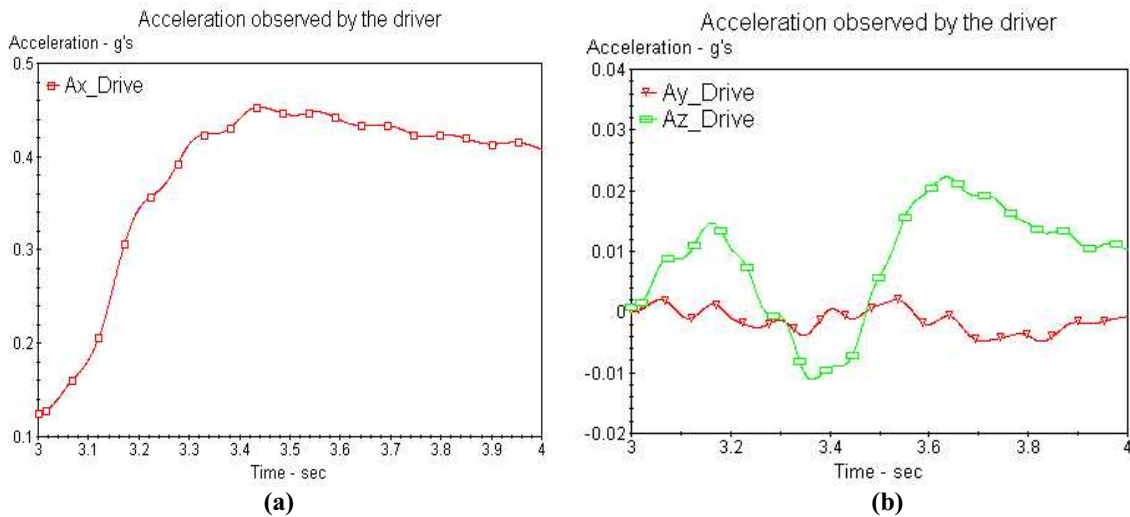(a)   (b)

FIGURE 14 Tip-in response at the driver's location, (a) longitudinal (b) vertical and lateral

Straight Forward – over Single Bump

Another example is the simulation of the car running straight over a 20mm high single bump on the left wheel at a constant speed (20m/s). Fig. 15 illustrates the trapezoidal shaped bump with a 0.3m span. Fig. 16 shows the acceleration response at the driver's location. Table 4 below describes the simulation parameters and simulation speed performances. For the reasons described above, the simulation is easily capable of running in real-time.

TABLE 4 Simulation Parameters and Speed Performances

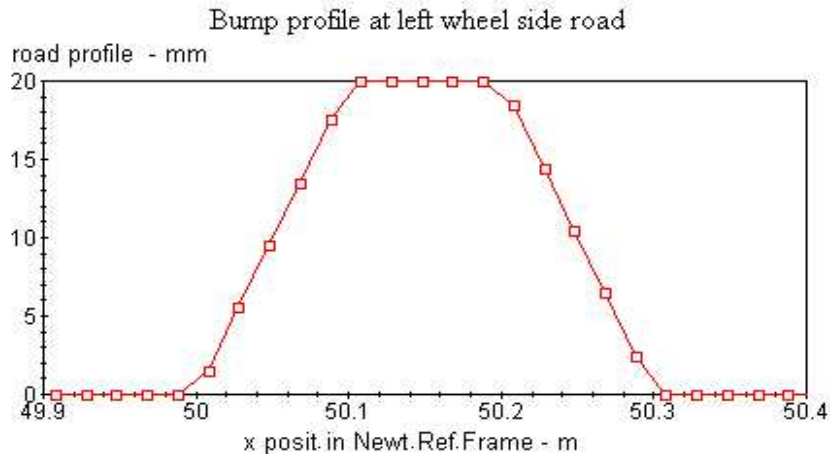|	
Speed	20m/s
Simulation Time Span	4s
Integration Step Size	0.001s
Road profile	Right wheel side: flat Left wheel side: single bump
Simulation Platform	Dell PC, PIII 700MHz, Windows 2000 OS
Simulation Speed	1.4s CPU Time for per Simulated Second

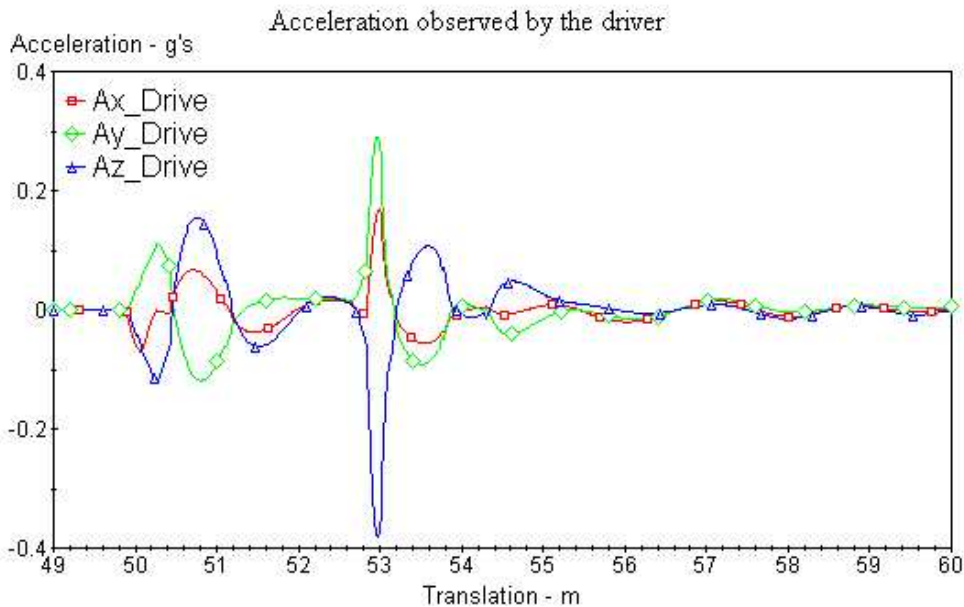**FIGURE 15 Road profile at left wheel side**

FIGURE 16 Driving over a single bump, accelerations at the driver's location

Parametric Study

In previous section, we discussed the dynamic responses of the example car for a tip-in application and the response when the car drove over a single bump at constant speed. For these two scenarios, parametric studies were performed to examine the influence of the vehicle response to changes in the powertrain natural frequencies. Assuming the mode shapes remained unchanged, three cases were compared: 1) all the natural frequencies were increased together by 20%, 2) all the natural frequencies were decreased together by 20%, and 3) baseline model. Fig. 17 shows the effect of various natural frequencies on vertical acceleration at the driver during throttle tip in. The large magnitude low-frequency oscillation can be attributed to the sprung mass roll mode being excited by the powertrain roll. The small fluctuations in the response are caused by vibration of the powertrain on the mounts. Fig. 17 shows that decreasing the powertrain natural frequencies values tends to increase the acceleration peak value. Figs. 18 through 20 exhibit the sensitivity of vehicle acceleration at the driver's location to the changes in powertrain natural frequencies when the vehicle passes over a single bump. These figures show little sensitivity to changes in powertrain natural frequencies for the initial response. However there appears to be some sensitivity to the parameter changes in the free response.
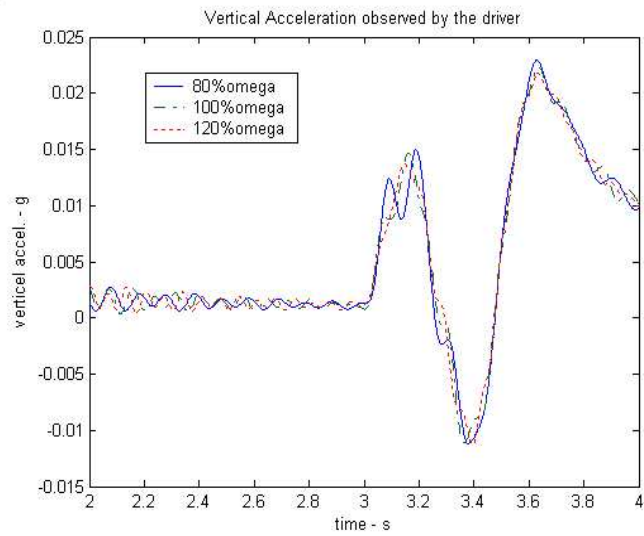
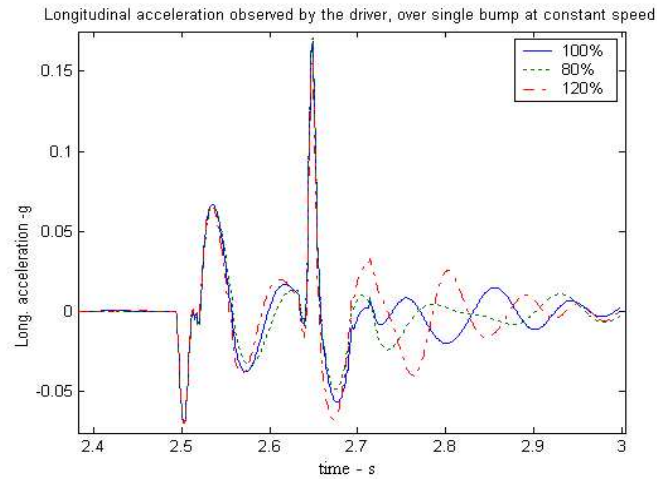**FIGURE 17 Vertical acceleration at the driver's location – throttle tip in**

FIGURE 18 Longitudinal acceleration at the driver's location – over single bump
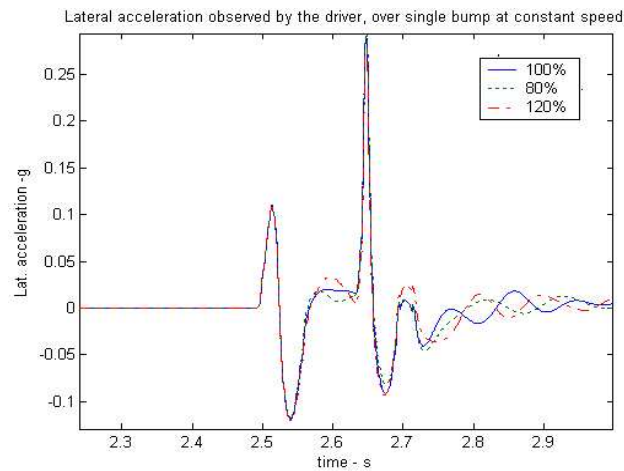

FIGURE 19 Lateral acceleration at the driver's location – over single bump
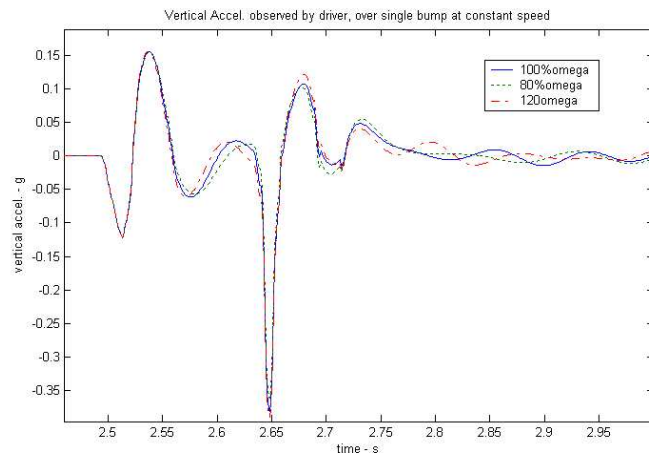
FIGURE 20 Vertical acceleration at the driver's location – over single bump

CONCLUSION

A powertrain model for real-time vehicle simulation was presented. The paper briefly describes the vehicle dynamics model, powertrain rigid body, and the torsional dynamics model. Modal superposition was used to implement the rigid body powertrain dynamics into the vehicle model. The powertrain torque/speed model generates the drive torques for the tire and the reaction moments acting on the powertrain body. The engine, torque converter, transmission, and differential all contribute to this part of the model. Simulations of an example car accelerating straight ahead, tip in of throttle, and running over a bump were presented. The former example compared favorable to existing data. Parametric studies were carried out for the tip in and bump simulations and the responses showed some sensitivity to the changes engine mode natural frequencies. The vehicle model is also capable of real-time simulation on contemporary PC's.

The ultimate goal for this work is to develop a better model of the dynamics interactions that occur between the powertrain and vehicle. This will improve the accuracy of the vehicle dynamics model, particularly the ride response, and thus, provide a more realistic driving simulation. The model presented in this paper represents the first step. Modeling improvements under consideration include the addition of powertrain compliance and damping, and a more realistic representation of the coupling between the powertrain and the vehicle. The later will include a more representative drive shaft model that will feature inboard tripode joints and outboard Rzeppa joints.

ACKNOWLEDGEMENTS

REFERENCES

(1) Cook, R.D., Malkus, D.S., Plesha, M.E., Witt, R.J., Concepts and Applications of Finite Element Analysis, John Wiley and Sons, Inc., 2002

(2) AutoSim Reference Manual 2.5+, Mechanical Simulation Corporation, Ann Arbor, MI, 1997

(3) Greenberg, J.A., Park T. and Mousseau C.W., Design and Analysis of the Ford Driving Simulator, Proceedings of the 1992 Image Conference.

(4) Sayers, M.W., and Mousseau C.W., Real-time Dynamic Simulation Obtained with a Symbolic Multibody Program, Transportation Systems, pp. 51-58, ASME, 1990.

(5) Mousseau, C.W., Markale, G., Obstacle Impact Simulation of an ATV using an Efficient Tire Model, submitted for publication in the Journal of Tire Science and Technology

(6) Bakker, E., Pacejka, H.B. and Linder, L., A New Tire Model with an Application in Vehicle Dynamics Studies, SAE Paper 890087, 1989

(7) Bernard, J.E., Clover, C.L., Tire Modeling for Low-Speed and High-Speed Calculations, SAE Paper 950311, 1995

(8) Clover, C.L., Bernard, J.E., Longitudinal Tire Dynamics, Vehicle System Dynamics, V29#4, April 1998, p231-259

(9) Greenwood, D.T., Principles of Dynamics, Prentice-Hall, Inc., 1988

(10) Wamsler, M., Rose, T., Advanced Mode Shape Identification Method for Automotive Application via Modal Kinetic Energy Plots Assisted by Numerous Printed Outputs, MSC American Users' Conference Proceedings, 1998

(11) Salaani, M.K., Heydinger, G.L., Powertrain and Brake Modeling of the 1994 Ford Taurus for the National Advanced Driving Simulator, SAE Paper 981190, 1998

(12) CarSim User Manual Ver. 5, Mechanical Simulation Corporation, Ann Arbor, MI, 2001

(13) Petrone, F., Fichera, G., and Lacagnina,M., A Numerical Model to Analyze the Dynamic Reponse of a Vehicle to Variations in Torque Transmitted by the Drive-line, SAE Paper 2001-01-3334, 2001